Simultaneous disappearances of plasmaspheric hiss, exohiss, and chorus waves triggered by a sudden decrease in solar wind dynamic pressure

Liu, N.; Su, Z.; Gao, Z.; Zheng, H.; Wang, Y.; Wang, S.; Spence, H. E.; Reeves, Geoffrey D.; Baker, D. N.; Blake, J. B.; Funsten, Herbert O.; Wygant, J. R.

To be published in: Geophysical Research Letters

DOI to publisher's version: 10.1002/2016GL071987

Simultaneous disappearances of plasmaspheric hiss, exohiss and chorus waves triggered by a solar wind negative pressure pulse

Nigang Liu,[1,2,3] Zhenpeng Su,[1,2] Zhonglei Gao,[1,2,3] Huinan Zheng,[1,2] Yuming Wang,[1] Shui Wang,[1] H. E. Spence,[4] G. D. Reeves,[5,6] D. N. Baker,[7] J. B. Blake,[8] H. O. Funsten,[9] and J. R. Wygant[10]

Z. Su, Department of Geophysics and Planetary Sciences, University of Science and Technology of China, Hefei, Anhui 230026, China. (szpe@mail.ustc.edu.cn)

[1]CAS Key Laboratory of Geospace Environment, Department of Geophysics and Planetary

Key Points.

- First report of simultaneous disappearances of plasmaspheric hiss, exohiss and chorus triggered by a solar wind negative pressure pulse
- Disappearance of chorus caused by the increase of dayside magnetic field inhomogeneity rather than the change of local electron free energy
- Disappearances of plasmaspheric hiss and exohiss resulting from the chorus quenching rather than the change of local plasma condition

Sciences, University of Science and Technology of China, Hefei, Anhui 230026, China

[2]Collaborative Innovation Center of Astronautical Science and Technology, China

[3]Mengcheng National Geophysical Observatory, School of Earth and Space Sciences, University of Science and Technology of China, Hefei, China

[4]Institute for the Study of Earth, Oceans, and Space, University of New Hampshire, Durham, New Hampshire, USA

[5]Space Science and Applications Group, Los Alamos National Laboratory, Los Alamos, New Mexico, USA

[6]Space Sciences Division, New Mexico Consortium, Los Alamos, New Mexico, USA

[7]Laboratory for Atmospheric and Space Physics, University of Colorado Boulder, Colorado, USA

[8]The Aerospace Corporation, Los Angeles, California, USA

[9]ISR Division, Los Alamos National Laboratory, Los Alamos, New Mexico, USA

[10]School of Physics and Astronomy, University of Minnesota, Minneapolis, Minnesota, USA

Magnetospheric whistler-mode waves are of great importance in the radiation belt electron dynamics. Here, on the basis of the analysis of a rare event with the simultaneous disappearances of whistler-mode plasmaspheric hiss, exohiss and chorus triggered by a solar wind negative pressure pulse, we provide evidences for the following physical scenarios: (1) nonlinear generation of chorus controlled by the geomagnetic field inhomogeneity, (2) origination of plasmaspheric hiss from chorus, and (3) leakage of plasmaspheric hiss into exohiss. After the solar wind negative pressure pulse, the dayside geomagnetic field configuration with the enhanced inhomogeneity became unfavored for the generation of chorus, and the quenching of chorus directly caused the disappearances of plasmaspheric hiss and then exohiss.

1. Introduction

Whistler-mode emission plays an important role in the acceleration [e.g., *Summers et al.*, 2002; *Horne et al.*, 2005; *Reeves et al.*, 2013; *Thorne et al.*, 2013a; *Su et al.*, 2014a, b; *Yang et al.*, 2016] and loss [e.g., *Lyons and Thorne*, 1973; *Abel and Thorne*, 1998; *Albert*, 1994; *Su et al.*, 2011a, 2016; *Thorne et al.*, 2013b; *Ni et al.*, 2014; *Baker et al.*, 2014; *Breneman et al.*, 2015; *Zhu et al.*, 2015; *He et al.*, 2016] of radiation belt electrons through cyclotron resonant interaction [*Kennel and Engelmann*, 1966; *Horne and Thorne*, 1998; *Summers et al.*, 1998]. Whistler-mode hiss is often observed as a structureless and incoherent band with the frequency ranging from ∼0.1 kHz to several kHz [*Russell et al.*, 1969; *Thorne et al.*, 1973; *Hayakawa and Sazhin*, 1992; *Summers et al.*, 2008]. According to the spatial location, whistler-mode hiss is divided into plasmaspheric hiss (inside the high-density plasmasphere and plasmaspheric plume) and exohiss (outside the plasmasphere) [*Russell et al.*, 1969; *Thorne et al.*, 1973]. Whistler-mode chorus is usually characterized as a structured and discrete emission in the frequency range from 0.1–0.8 $f_{\mathrm{ce\_eq}}$ ($f_{\mathrm{ce\_eq}}$ is the equatorial electron gyro-frequency) outside the plasmasphere [*Tsurutani and Smith*, 1974, 1977; *Meredith et al.*, 2001; *Santolík et al.*, 2003]. Recently, the low-frequency plasmaspheric hiss ($\sim$ 10 Hz) [*Li et al.*, 2013] and chorus ($< 0.1\ f_{\mathrm{ce\_eq}}$) [*Cattell et al.*, 2015; *Gao et al.*, 2016] have been detected following the substorm injection or during the geomagnetic storm.

Generation mechanisms of these whistler-mode waves are of great interest in the radiation belt community. For plasmaspheric hiss, there have been two main candidate mechanisms: excitation by electron cyclotron instability in the outer plasmasphere [e.g., *Thorne et al.*, 1979; *Chen et al.*, 2014; *Summers et al.*, 2014] and origination from chorus outside the plasmasphere [*Bortnik et al.*, 2008, 2009; *Li et al.*, 2015]. A possible scenario for exohiss is that plasmaspheric hiss leaks from the plasmasphere and evolves into exohiss in the plasmatrough [*Thorne et al.*, 1973; *Bortnik et al.*, 2008; *Zhu et al.*, 2015]. Chorus is generally believed to be excited through the cyclotron resonance with anisotropic suprathermal (from a few keV to tens of keV) electrons [e.g., *Kennel and Engelmann*, 1966; *Li et al.*, 2009; *Su et al.*, 2014c] near the magnetic equator [e.g., *LeDocq et al.*, 1998] in the plasmatrough. In particular, the nonlinear resonance process has been proposed to explain the frequency-time characteristics of chorus [e.g., *Nunn et al.*, 1997; *Omura et al.*, 2008; *Katoh and Omura*, 2013; *Nunn and Omura*, 2015]. In this letter, we give the first report on the simultaneous disappearances of plasmaspheric hiss, exohiss and chorus triggered by a solar wind negative pressure pulse. This impulsive event was monitored by the Van Allen Probes (RBSP) mission [*Mauk et al.*, 2013] and the Time History of Events and Macroscale Interactions during Substorm (THEMIS) mission [*Angelopoulos*, 2008] both inside and outside the plasmasphere, offering a rare opportunity to test the generation mechanisms of these whistler-mode waves.

2. Data and Instrumentation

Geomagnetic activity indices are obtained from the World Data Center for Geomagnetism, Kyoto. Interplanetary parameters at 1 AU are provided by the OMNI database of CDAweb [*King and Papitashvili*, 2005]. In the OMNI database, the measured solar wind data sets had been time-shifted to the Earth's bow shock nose.

The RBSP is a twin-satellite mission to study the Van Allen radiation belt dynamics. Background magnetic field and wave power spectral density were directly measured by the Electric and Magnetic Field Instrument Suite and Integrated Science (EMFISIS) suite [*Kletzing et al.*, 2013]. Electric field was detected by the Electric Field and Waves (EFW) [*Wygant et al.*, 2013] instrument. Suprathermal and energetic electron fluxes were observed by the Helium Oxygen Proton Electron (HOPE) Mass Spectrometer [*Funsten et al.*, 2013] and the Magnetic Electron Ion Spectrometer (MagEIS) [*Blake et al.*, 2013] of the Energetic Particle, Composition, and Thermal Plasma (ECT) Suite [*Spence et al.*, 2013]. Background electron density can be derived from the upper hybrid resonance frequency measured by EMFISIS [*Kurth et al.*, 2014].

The THEMIS mission contains five satellites to study the energy releases of magnetospheric substorms [*Angelopoulos et al.*, 2008]. Background magnetic and electric fields were detected by the Fluxgate Magnetometer (FGM) [*Auster et al.*, 2008] and the Electric Field Instrument (EFI) [*Bonnell et al.*, 2008]. Wave power spectral density was measured by the Search Coil Magnetometer (SCM) [*Le Contel et al.*, 2008]. Suprathermal and energetic electron fluxes were observed by the Electrostatic Analyzer (ESA) [*McFadden et al.*, 2008] and the Solid State Telescope (SST) [*Angelopoulos*, 2008]. Background electron density can be estimated from the spacecraft potential and the electron thermal speed [*Li et al.*, 2010] measured by EFI and ESA.

3. Event overview

Figure 1 shows a schematic diagram of the magnetospheric structures and the orbits of RBSP and THEMIS missions on 12 February 2014. The magnetopause location is estimated from the interplanetary parameters on the basis of the previous statistical model [*Shue et al.*, 1998]. The plasmasphere configuration is roughly determined on the basis of the available density observations and the numerical simulations of *Goldstein et al.* [2014]. The plasmaspheric plume formed in the time period from 18:00 UT to 24:00 UT on 11 February 2014 with the southward interplanetary magnetic field. The apogees of RBSP-A, RBSP-B and TH-E satellites were located in the afternoon sector of the magnetosphere.

Figure 2 gives an overview of the wave disappearance event observed by RBSP-A, RBSP-B and TH-E satellites in the time range from 03:00 UT to 08:00 UT on 12 February 2014. Throughout this event, the magnetosphere (with SYM-H> -25 nT and AE$<$ 250 nT) was free from both magnetic storms and substorms. Around 04:00 UT, the magnetosphere encountered a solar wind negative pressure pulse (with a prompt decrease of SYM-H from 5 nT to -23 nT) and the subsolar magnetopause expanded from 11 R_{E} to 12 R_{E}. In response to this pulse, exohiss waves detected by RBSP-A, plasmaspheric hiss waves detected by RBSP-B and chorus waves detected by TH-E disappeared simultaneously within the comparable frequency range 0.2–0.4 kHz. Note that the magnetosonic waves below 0.2 kHz were continuously observed by RBSP-A both before and after the pulse. Around 04:30 UT, RBSP-A went into the plasmasphere and began to observe the plasmaspheric hiss waves. Because of the smooth variation of cold electron density measured by RBSP-B, the plasmapause location was hard to be determined accurately. Roughly speaking, RBSP-B detected plasmaspheric hiss waves during 04:30-05:00 UT, exohiss waves during 05:00-08:00 UT and chorus waves after 06:30 UT. TH-E satellite re-observed chorus waves after 05:30 UT. In contrast to the wave disappearances, the recoveries of whistler-mode waves observed by the three satellites had no clear correspondence to each other, primarily due to the highly scattered satellite locations and the absence of interplanetary triggers and global magnetospheric processes (e.g., substorms).

4. Physical explanations

4.1. Disappearances of plasmaspheric hiss and exohiss

Figure 3 plots the suprathermal electron fluxes and electromagnetic fields observed by twin RBSP satellites around the pulse time. The local variation of magnetic field behaved similarly to the SYM-H index in both shape and magnitude. The electric field disturbance reached ∼1 mV/m at high L-shells (RBSP-A) but became nearly invisible at low L-shells (RBSP-B). The compression of magnetosphere (corresponding to the peak of SYM-H index) increased the suprathermal electron anisotropy during a short time period both inside and outside the plasmasphere. After the pulse, the electron fluxes of RBSP-A near the loss cone were decreased to some extent, which would increase the corresponding electron anisotropy and then the local growth rate of whistler-mode waves. In contrast, for RBSP-B, there were no significant differences between electron fluxes before and after the SYM-H peak. These results suggest that the generations/disappearances of plasmaspheric hiss and exohiss were not predominantly controlled by the local physical processes. Origination of plasmaspheric hiss from chorus [*Bortnik et al.*, 2008, 2009; *Li et al.*, 2015] and leakage of plasmaspheric hiss into exohiss [*Thorne et al.*, 1973; *Bortnik et al.*, 2008; *Zhu et al.*, 2015] may be two appropriate prerequisites to explain this impulsive event. As shown in the previous ray-tracing simulations [*Chen et al.*, 2009], chorus originating from a broad dayside region can propagate into the plasmasphere and plasmaspheric hiss can propagate both azimuthally and radially over a wide spatial region. As a result, although the wave observations were available only at three satellite locations, the three types of whistler-mode waves can still be expected to disappear over a vast region of dayside magnetosphere. In the last analysis, the disappearances of plasmaspheric hiss and exohiss may be simply attributed to the disappearance of chorus for this event.

4.2. Disappearance of chorus

As illustrated in the previous quasilinear [e.g., *Kennel and Engelmann*, 1966; *Li et al.*, 2009; *Su et al.*, 2014c] and nonlinear [e.g., *Nunn et al.*, 1997; *Omura et al.*, 2008; *Katoh and Omura*, 2013; *Nunn and Omura*, 2015] simulations, the growth of chorus is largely controlled by the free energy of resonant electrons and the inhomogeneity of background magnetic field. The former is mainly determined by the ratio between plasma frequency and electron gyrofrequency $f_{\rm pe}/f_{\rm ce}$ and the suprathermal electron phase space density F, and the latter is characterized by the magnetic field curvature Q.

Figure 4 shows the ratio between plasma frequency and electron gyrofrequency $f_{\rm pe}/f_{\rm ce}$ for TH-E satellite around the pulse time. With the expansion of magnetosphere, the ambient magnetic field decreased from 70 nT to 45 nT while the estimated electron density remained a quite low value (less than 1 cm^{-3}). Correspondingly, the parameter $f_{\rm pe}/f_{\rm ce}$ increased from 3.0 to 4.5 and the minimum resonant energy $E_{\rm min}$ [*Summers et al.*, 2007] of chorus waves at the central frequency 0.25 kHz decreased from over 60 keV to about 30 keV. Figure 5 presents the electron phase space densities F measured by TH-E satellite around the pulse time. As time went on, the electron phase space densities had some fluctuations. However, there were no significant differences between electron phase space densities before and after the pulse. These results suggest that the observed variations of $f_{\mathrm{pe}}/f_{\mathrm{ce}}$ and F could increase the free energy for chorus wave growth after the pressure pulse and were unlikely to cause the chorus quenching.

Figure 6 shows the evolution of geomagnetic field configuration around the pulse time. Before the pulse, TH-E satellite was roughly in the "dayside uniform zone" with a relatively small magnetic field line curvature $Q \sim< 0.1\ R_{\mathrm{E}}^{-1}$. The dayside uniform zone [*Keika et al.*, 2012] has been characterized as a transition region between the dipolar zone of the inner magnetosphere to the double minimum-B zone near the dayside magnetopause [*Tsurutani et al.*, 2009]. After the pulse, the dayside magnetosphere expanded outward and the geomagnetic field curvature Q for TH-E satellite increased by $\sim$0.1 R_{E}^{-1}. The increase of field line curvature would enhance the magnetic mirror force on resonant electrons and then reduce the nonlinearity of cyclotron resonance, not conductive to the nonlinear growth of chorus waves [*Omura et al.*, 2008; *Katoh and Omura*, 2013]. These results suggest that the dominant cause of chorus disappearance may be the increase of ambient magnetic field inhomogeneity in this event.

5. Discussion and Conclusion

Whistler-mode waves are commonly considered to contribute significantly to the radiation belt electron dynamics [see review by *Thorne*, 2010]. Spatiotemporal distribution information of these whistler-mode waves is required to develop global radiation belt models [e.g., *Varotsou et al.*, 2005, 2008; *Fok et al.*, 2008; *Shprits et al.*, 2009; *Subbotin et al.*, 2010; *Su et al.*, 2010, 2011b; *Tu et al.*, 2013; *Glauert et al.*, 2014]. Many previous studies focused on the statistical dependence of whistler-mode waves on geomagnetic activity indices and solar wind parameters [e.g., *Meredith et al.*, 2004, 2014; *Li et al.*, 2011; *Golden et al.*, 2012; *Agapitov et al.*, 2013; *Tsurutani et al.*, 2014]. In recent years, the prompt responses of magnetospheric whistler-mode waves to interplanetary disturbances have received increasing attention. Disappearance of plasmaspheric hiss [*Su et al.*, 2015] and intensification of chorus [*Fu et al.*, 2012; *Zhou et al.*, 2015] induced by interplanetary shocks have been reported. In this letter, we present the first report of simultaneous disappearances of plasmaspheric hiss, exohiss and chorus triggered by a solar wind negative pressure pulse. In contrast to the shock-induced disappearance of plasmaspheric hiss over about 5 h [*Su et al.*, 2015], the disappearances of plasmaspheric hiss, exohiss and chorus reported here lasted only about 0.5 h. Such difference in time duration may be related to the difference in the magnetospheric disturbance intensity. However, the disappearances of whistler-mode waves in both events were likely to occur over a vast region of dayside magnetosphere. Our present report, together with the previous studies mentioned above, highlight the considerable and complex variability of magnetospheric whistler-mode waves.

Investigation of the prompt response of whistler-mode waves to interplanetary disturbances can help us to better understand the wave generation mechanisms. In this impulsive event on 12 February 2014, three satellites from RBSP and THEMIS missions were able to simultaneously monitor the responses of plasmas and waves both inside and outside the plasmasphere to the interplanetary disturbance. The disappearance of chorus is suggested to be mainly caused by the increase of dayside magnetic field inhomogeneity [*Omura et al.*, 2008; *Katoh and Omura*, 2013], rather than the potential change of local electron free energy. A large curvature of the background magnetic field line was not conducive to the nonlinear growth of chorus waves [*Omura et al.*, 2008; *Katoh and Omura*, 2013; *Tao et al.*, 2014]. The underlying physical process in this negative pressure pulse event may be treated as an "inverse" process acting in the shock event [*Zhou et al.*, 2015]. As shown in the previous statistical studies [*Zhou et al.*, 2015], interplanetary shocks could compress the magnetosphere, reduce the magnetic field line curvature by ∼0.1 R_E^{-1} and then promote the excitation of chorus waves. The disappearances of plasmaspheric hiss and exohiss are found to be not a result of the local plasma changes in this specific event. Origination of plasmaspheric hiss from chorus [*Bortnik et al.*, 2008, 2009; *Li et al.*, 2015] and leakage of plasmaspheric hiss into exohiss [*Thorne et al.*, 1973; *Bortnik et al.*, 2008; *Zhu et al.*, 2015] may be two appropriate prerequisites to explain this event. The disappearances of plasmaspheric hiss and exohiss should be ultimately attributed to the quenching of chorus.

Acknowledgments. This work was supported by the National Natural Science Foundation of China grants 41631071, 41422405, 41274169, 41274174, 41174125, 41131065, 41421063, 41231066 and 41304134, the Chinese Academy of Sciences grant KZCX2-EW-QN510 and KZZD-EW-01-4, the CAS Key Research Program of Frontier Sciences grant QYZDB-SSW-DQC015, the National Key Basic Research Special Foundation of China Grant No. 2011CB811403, and the Fundamental Research Funds for the Central Universities WK2080000077. We acknowledge J. H. King, N. Papatashvilli, and CDAWeb for the use of interplanetary parameters and magnetospheric indices, acknowledge the University of Iowa as the source for the EMFISIS data (this acknowledgement does not imply endorsement of the publication by the University of Iowa or its researchers), and acknowledge THEMIS team for the use of SCM, FGM, ESA, SST and EFI data. The interplanetary parameters and geomagnetic indices are obtained at the CDAWeb (http://cdaweb.gsfc.nasa.gov/cdaweb/istp_public/). The RBSP data are available at the websites (http:// emfisis.physics.uiowa.edu/Flight/ for EMFISIS, http://www.rbsp-ect.lanl.gov/data_pub/ for ECT and http://www.space.umn.edu/rbspefw-data/ for EFW). The THEMIS data are available at the website (http://themis.ssl.berkeley.edu/data/themis/).

References

Abel, B., and R. M. Thorne (1998), Electron scattering loss in Earth's inner magnetosphere 1. Dominant physical processes, *J. Geophys. Res.*, *103*, 2385–2396, doi: 10.1029/97JA02919.

Agapitov, O., A. Artemyev, V. Krasnoselskikh, Y. V. Khotyaintsev, D. Mourenas, H. Breuillard, M. Balikhin, and G. Rolland (2013), Statistics of whistler mode waves in the outer radiation belt: Cluster STAFF-SA measurements, *J. Geophys. Res.*, *118*, 3407–3420, doi:10.1002/jgra.50312.

Albert, J. M. (1994), Quasi-linear pitch angle diffusion coefficients: Retaining high harmonics, *J. Geophys. Res.*, *99*, 23,741, doi:10.1029/94JA02345.

Angelopoulos, V. (2008), The THEMIS Mission, *Space Sci. Rev.*, *141*, 5–34, doi: 10.1007/s11214-008-9336-1.

Angelopoulos, V., D. Sibeck, C. W. Carlson, J. P. McFadden, D. Larson, R. P. Lin, J. W. Bonnell, F. S. Mozer, R. Ergun, C. Cully, K. H. Glassmeier, U. Auster, A. Roux, O. Lecontel, S. Frey, T. Phan, S. Mende, H. Frey, E. Donovan, C. T. Russell, R. Strangeway, J. Liu, I. Mann, J. Rae, J. Raeder, X. Li, W. Liu, H. J. Singer, V. A. Sergeev, S. Apatenkov, G. Parks, M. Fillingim, and J. Sigwarth (2008), First Results from the THEMIS Mission, *Space Sci. Rev.*, *141*, 453–476, doi:10.1007/s11214-008-9378-4.

Auster, H. U., K. H. Glassmeier, W. Magnes, O. Aydogar, W. Baumjohann, D. Constantinescu, D. Fischer, K. H. Fornacon, E. Georgescu, P. Harvey, O. Hillenmaier, R. Kroth, M. Ludlam, Y. Narita, R. Nakamura, K. Okrafka, F. Plaschke, I. Richter, H. Schwarzl, B. Stoll, A. Valavanoglou, and M. Wiedemann (2008), The THEMIS Fluxgate Magnetometer, *Space Sci. Rev.*, *141*, 235–264, doi:10.1007/s11214-008-9365-9.

Baker, D. N., A. N. Jaynes, V. C. Hoxie, R. M. Thorne, J. C. Foster, X. Li, J. F. Fennell, J. R. Wygant, S. G. Kanekal, P. J. Erickson, W. Kurth, W. Li, Q. Ma, Q. Schiller, L. Blum, D. M. Malaspina, A. Gerrard, and L. J. Lanzerotti (2014), An impenetrable barrier to ultrarelativistic electrons in the Van Allen radiation belts, *Nature*, *515*, 531–534, doi:10.1038/nature13956.

Blake, J. B., P. A. Carranza, S. G. Claudepierre, J. H. Clemmons, W. R. Crain, Y. Dotan, J. F. Fennell, F. H. Fuentes, R. M. Galvan, J. S. George, M. G. Henderson, M. Lalic, A. Y. Lin, M. D. Looper, D. J. Mabry, J. E. Mazur, B. McCarthy, C. Q. Nguyen, T. P. O'Brien, M. A. Perez, M. T. Redding, J. L. Roeder, D. J. Salvaggio, G. A. Sorensen, H. E. Spence, S. Yi, and M. P. Zakrzewski (2013), The magnetic electron ion spectrometer (MagEIS) instruments aboard the radiation belt storm probes (RBSP) spacecraft, *Space Sci. Rev.*, *179*, 383–421, doi:10.1007/s11214-013-9991-8.

Bonnell, J. W., F. S. Mozer, G. T. Delory, A. J. Hull, R. E. Ergun, C. M. Cully, V. Angelopoulos, and P. R. Harvey (2008), The Electric Field Instrument (EFI) for THEMIS, *Space Sci. Rev.*, *141*, 303–341, doi:10.1007/s11214-008-9469-2.

Bortnik, J., R. M. Thorne, and N. P. Meredith (2008), The unexpected origin of plasmaspheric hiss from discrete chorus emissions, *Nature*, *452*, 62–66, doi:10.1038/nature06741.

Bortnik, J., W. Li, R. M. Thorne, V. Angelopoulos, C. Cully, J. Bonnell, O. Le Contel, and A. Roux (2009), An observation linking the origin of plasmaspheric hiss to discrete chorus emissions, *Science*, *324*, 775, doi:10.1126/science.1171273.

Breneman, A., A. Halford, R. Millan, M. McCarthy, J. Fennell, J. Sample, L. Woodger, G. Hospodarsky, J. Wygant, C. Cattell, J. Goldstein, D. Malaspina, and C. Kletzing (2015), Global-scale coherence modulation of radiation-belt electron loss from plasmaspheric hiss, *Nature*, *523*, 193–195, doi:10.1038/nature14515.

Cattell, C. A., A. W. Breneman, S. A. Thaller, J. R. Wygant, C. A. Kletzing, and W. S. Kurth (2015), Van Allen Probes observations of unusually low frequency whistler mode waves observed in association with moderate magnetic storms: Statistical study, *Geophys. Res. Lett.*, *42*, 7273–7281, doi:10.1002/2015GL065565.

Chen, L., J. Bortnik, R. M. Thorne, R. B. Horne, and V. K. Jordanova (2009), Three-dimensional ray tracing of VLF waves in a magnetospheric environment containing a plasmaspheric plume, *Geophys. Res. Lett.*, *36*, L22101, doi:10.1029/2009GL040451.

Chen, L., R. M. Thorne, J. Bortnik, W. Li, R. B. Horne, G. D. Reeves, C. A. Kletzing, W. S. Kurth, G. B. Hospodarsky, H. E. Spence, J. B. Blake, and J. F. Fennell (2014), Generation of unusually low frequency plasmaspheric hiss, *Geophys. Res. Lett.*, *41*, 5702–5709, doi:10.1002/2014GL060628.

Fok, M.-C., R. B. Horne, N. P. Meredith, and S. A. Glauert (2008), Radiation Belt Environment model: Application to space weather nowcasting, *J. Geophys. Res.*, *113*(A12), A03S08, doi:10.1029/2007JA012558.

Fu, H. S., J. B. Cao, F. S. Mozer, H. Y. Lu, and B. Yang (2012), Chorus intensification in response to interplanetary shock, *J. Geophys. Res.*, *117*, A01203, doi:10.1029/2011JA016913.

Funsten, H. O., R. M. Skoug, A. A. Guthrie, E. A. MacDonald, J. R. Baldonado, R. W. Harper, K. C. Henderson, K. H. Kihara, J. E. Lake, B. A. Larsen, A. D. Puckett, V. J. Vigil, R. H. Friedel, M. G. Henderson, J. T. Niehof, G. D. Reeves, M. F. Thomsen, J. J. Hanley, D. E. George, J.-M. Jahn, S. Cortinas, A. De Los Santos, G. Dunn, E. Edlund, M. Ferris, M. Freeman, M. Maple, C. Nunez, T. Taylor, W. Toczynski, C. Urdiales, H. E. Spence, J. A. Cravens, L. L. Suther, and J. Chen (2013), Helium, Oxygen, Proton, and Electron (HOPE) Mass Spectrometer for the Radiation Belt Storm Probes Mission, *Space Sci. Rev.*, *179*, 423–484, doi:10.1007/s11214-013-9968-7.

Gao, Z., Z. Su, H. Zhu, F. Xiao, H. Zheng, Y. Wang, C. Shen, and S. Wang (2016), Intense low-frequency chorus waves observed by Van Allen Probes: Fine structures and potential effect on radiation belt electrons, *Geophys. Res. Lett.*, *43*, 967–977, doi:10.1002/2016GL067687.

Glauert, S. A., R. B. Horne, and N. P. Meredith (2014), Three-dimensional electron radiation belt simulations using the BAS Radiation Belt Model with new diffusion models for chorus, plasmaspheric hiss, and lightning-generated whistlers, *J. Geophys. Res.*, *119*, 268–289, doi:10.1002/2013JA019281.

Golden, D. I., M. Spasojevic, W. Li, and Y. Nishimura (2012), Statistical modeling of plasmaspheric hiss amplitude using solar wind measurements and geomagnetic indices, *Geophys. Res. Lett.*, *39*, L06103, doi:10.1029/2012GL051185.

Goldstein, J., S. D. Pascuale, C. Kletzing, W. Kurth, K. J. Genestreti, R. M. Skoug, B. A. Larsen, L. M. Kistler, C. Mouikis, and H. Spence (2014), Simulation of Van Allen Probes plasmapause encounters, *J. Geophys. Res.*, *119*, 7464–7484, doi:10.1002/2014JA020252.

Hayakawa, M., and S. S. Sazhin (1992), Mid-latitude and plasmaspheric hiss - A review, *Planet. Space Sci.*, *40*, 1325–1338, doi:10.1016/0032-0633(92)90089-7.

He, Z., Q. Yan, Y. Chu, and Y. Cao (2016), Wave-driven gradual loss of energetic electrons in the slot region, *J. Geophys. Res.*, *121*(9), 8614–8623, doi:10.1002/2016JA023087, 2016JA023087.

Horne, R. B., and R. M. Thorne (1998), Potential waves for relativistic electron scattering and stochastic acceleration during magnetic storms, *Geophys. Res. Lett.*, *25*, 3011–3014, doi:10.1029/98GL01002.

Horne, R. B., R. M. Thorne, Y. Y. Shprits, N. P. Meredith, S. A. Glauert, A. J. Smith, S. G. Kanekal, D. N. Baker, M. J. Engebretson, J. L. Posch, M. Spasojevic, U. S. Inan, J. S. Pickett, and P. M. E. Decreau (2005), Wave acceleration of electrons in the Van Allen radiation belts, *Nature*, *437*, 227–230, doi:10.1038/nature03939.

Katoh, Y., and Y. Omura (2013), Effect of the background magnetic field inhomogeneity on generation processes of whistler-mode chorus and broadband hiss-like emissions, *J. Geophys. Res.*, *118*, 4189–4198, doi:10.1002/jgra.50395.

Keika, K., M. Spasojevic, W. Li, J. Bortnik, Y. Miyoshi, and V. Angelopoulos (2012), PENGUIn/AGO and THEMIS conjugate observations of whistler mode chorus waves in the dayside uniform zone under steady solar wind and quiet geomagnetic conditions, *J. Geophys. Res.*, *117*, A07212, doi:10.1029/2012JA017708.

Kennel, C. F., and F. Engelmann (1966), Velocity space diffusion from weak plasma turbulence in a magnetic field, *Phys. Fluids*, *9*, 2377–2388, doi:10.1063/1.1761629.

King, J. H., and N. E. Papitashvili (2005), Solar wind spatial scales in and comparisons of hourly Wind and ACE plasma and magnetic field data, *J. Geophys. Res.*, *110*, A02104, doi:10.1029/2004JA010649.

Kletzing, C. A., W. S. Kurth, M. Acuna, R. J. MacDowall, R. B. Torbert, T. Averkamp, D. Bodet, S. R. Bounds, M. Chutter, J. Connerney, D. Crawford, J. S. Dolan, R. Dvorsky, G. B. Hospodarsky, J. Howard, V. Jordanova, R. A. Johnson, D. L. Kirchner, B. Mokrzycki, G. Needell, J. Odom, D. Mark, R. Pfaff, J. R. Phillips, C. W. Piker, S. L. Remington, D. Rowland, O. Santolik, R. Schnurr, D. Sheppard, C. W. Smith, R. M. Thorne, and J. Tyler (2013), The Electric and Magnetic Field Instrument Suite and Integrated Science (EMFISIS) on RBSP, *Space Sci. Rev.*, doi:10.1007/s11214-013-9993-6.

Kurth, W. S., S. D. Pascuale, J. B. Faden, C. A. Kletzing, G. B. Hospodarsky, S. Thaller, and J. R. Wygant (2014), Electron densities inferred from plasma wave spectra obtained by the waves instrument on van allen probes, *J. Geophys. Res.*, *120*, 904–914, doi:10.1002/2014JA020857.

Le Contel, O., A. Roux, P. Robert, C. Coillot, A. Bouabdellah, B. de La Porte, D. Alison, S. Ruocco, V. Angelopoulos, K. Bromund, C. C. Chaston, C. Cully, H. U. Auster, K. H. Glassmeier, W. Baumjohann, C. W. Carlson, J. P. McFadden, and D. Larson (2008), First Results of the THEMIS Search Coil Magnetometers, *Space Sci. Rev.*, *141*, 509–534, doi:10.1007/s11214-008-9371-y.

LeDocq, M. J., D. A. Gurnett, and G. B. Hospodarsky (1998), Chorus source locations from VLF poynting flux measurements with the polar spacecraft, *Geophys. Res. Lett.*, *25*, 4063–4066, doi:10.1029/1998GL900071.

Li, W., R. M. Thorne, V. Angelopoulos, J. W. Bonnell, J. P. McFadden, C. W. Carlson, O. LeContel, A. Roux, K. H. Glassmeier, and H. U. Auster (2009), Evaluation of whistler-mode chorus intensification on the nightside during an injection event observed on the THEMIS spacecraft, *J. Geophys. Res.*, *114*, A00C14, doi:10.1029/2008JA013554.

Li, W., R. M. Thorne, J. Bortnik, Y. Nishimura, V. Angelopoulos, L. Chen, J. P. McFadden, and J. W. Bonnell (2010), Global distributions of suprathermal electrons observed on THEMIS and potential mechanisms for access into the plasmasphere, *J. Geophys. Res.*, *115*, A00J10, doi:10.1029/2010JA015687.

Li, W., J. Bortnik, R. M. Thorne, and V. Angelopoulos (2011), Global distribution of wave amplitudes and wave normal angles of chorus waves using THEMIS wave observations, *J. Geophys. Res.*, *116*, A12205, doi:10.1029/2011JA017035.

Li, W., R. M. Thorne, J. Bortnik, G. D. Reeves, C. A. Kletzing, W. S. Kurth, G. B. Hospodarsky, H. E. Spence, J. B. Blake, J. F. Fennell, S. G. Claudepierre, J. R. Wygant, and S. A. Thaller (2013), An unusual enhancement of low-frequency plasmaspheric hiss in the outer plasmasphere associated with substorm-injected electrons, *Geophys. Res. Lett.*, *40*, 3798–3803, doi:10.1002/grl.50787.

Li, W., L. Chen, J. Bortnik, R. M. Thorne, V. Angelopoulos, C. A. Kletzing, W. S. Kurth, and G. B. Hospodarsky (2015), First evidence for chorus at a large geocentric distance as a source of plasmaspheric hiss: Coordinated THEMIS and Van Allen Probes observation, *Geophys. Res. Lett.,* , *42*, 241–248, doi:10.1002/2014GL062832.

Lyons, L. R., and R. M. Thorne (1973), Equilibrium structure of radiation belt electrons, *J. Geophys. Res.*, *78*, 2142–2149, doi:10.1029/JA078i013p02142.

Mauk, B. H., N. J. Fox, S. G. Kanekal, R. L. Kessel, D. G. Sibeck, and A. Ukhorskiy (2013), Science objectives and rationale for the Radiation Belt Storm Probes mission, *Space Sci. Rev.*, *179*, 3–27, doi:10.1007/s11214-012-9908-y.

McFadden, J. P., C. W. Carlson, D. Larson, J. Bonnell, F. Mozer, V. Angelopoulos, K.-H. Glassmeier, and U. Auster (2008), THEMIS ESA first science results and performance issues, *Space Sci. Rev.*, *141*, 477–508, doi:10.1007/s11214-008-9433-1.

Meredith, N. P., R. B. Horne, and R. R. Anderson (2001), Substorm dependence of chorus amplitudes: Implications for the acceleration of electrons to relativistic energies, *J. Geophys. Res.*, *106*, 13,165–13,178, doi:10.1029/2000JA900156.

Meredith, N. P., R. B. Horne, R. M. Thorne, D. Summers, and R. R. Anderson (2004), Substorm dependence of plasmaspheric hiss, *J. Geophys. Res.*, *109*, A06,209, doi:10.1029/2004JA010387.

Meredith, N. P., R. B. Horne, W. Li, R. M. Thorne, and A. Sicard-Piet (2014), Global model of low-frequency chorus ($f_{LHR} < f < 0.1 f_{ce}$) from multiple satellite observations, *Geophys. Res. Lett.*, , *41*, 280–286, doi:10.1002/2013GL059050.

Ni, B., W. Li, R. M. Thorne, J. Bortnik, Q. Ma, L. Chen, C. A. Kletzing, W. S. Kurth, G. B. Hospodarsky, G. D. Reeves, H. E. Spence, J. Bernard Blake, J. F. Fennell, and S. G. Claudepierre (2014), Resonant scattering of energetic electrons by unusual low-frequency hiss, *Geophys. Res. Lett.*, *41*, 1854–1861, doi:10.1002/2014GL059389.

Nunn, D., and Y. Omura (2015), A computational and theoretical investigation of non-linear wave-particle interactions in oblique whistlers, *J. Geophys. Res.*, *120*, 2890–2911, doi:10.1002/2014JA020898.

Nunn, D., Y. Omura, H. Matsumoto, I. Nagano, and S. Yagitani (1997), The numerical simulation of VLF chorus and discrete emissions observed on the geotail satellite using a Vlasov code, *J. Geophys. Res.*, *102*, 27,083–27,098, doi:10.1029/97JA02518.

Omura, Y., Y. Katoh, and D. Summers (2008), Theory and simulation of the generation of whistler-mode chorus, *J. Geophys. Res.*, *113*, A04223, doi:10.1029/2007JA012622.

Reeves, G. D., H. E. Spence, M. G. Henderson, S. K. Morley, R. H. W. Friedel, H. O. Funsten, D. N. Baker, S. G. Kanekal, J. B. Blake, J. F. Fennell, et al. (2013), Electron acceleration in the heart of the van allen radiation belts, *Science*, *341*(6149), 991–994, doi:10.1126/science.1237743.

Russell, C. T., R. E. Holzer, and E. J. Smith (1969), OGO 3 observations of ELF noise in the magnetosphere. 1. Spatial extent and frequency of occurrence, *J. Geophys. Res.*, *74*, 755–777, doi:10.1029/JA074i003p00755.

Santolík, O., D. A. Gurnett, J. S. Pickett, M. Parrot, and N. Cornilleau-Wehrlin (2003), Spatio-temporal structure of storm-time chorus, *J. Geophys. Res.*, *108*, 1278, doi:

10.1029/2002JA009791.

Shprits, Y. Y., D. Subbotin, and B. Ni (2009), Evolution of electron fluxes in the outer radiation belt computed with the VERB code, *J. Geophys. Res.*, *114*, A11,209, doi: 10.1029/2008JA013784.

Shue, J., P. Song, C. T. Russell, J. T. Steinberg, J. K. Chao, G. Zastenker, O. L. Vaisberg, S. Kokubun, H. J. Singer, T. R. Detman, and H. Kawano (1998), Magnetopause location under extreme solar wind conditions, *J. Geophys. Res.*, *103*, 17,691–17,700, doi:10.1029/98JA01103.

Spence, H. E., G. D. Reeves, D. N. Baker, J. B. Blake, M. Bolton, S. Bourdarie, A. H. Chan, S. G. Claudepierre, J. H. Clemmons, J. P. Cravens, S. R. Elkington, J. F. Fennell, R. H. W. Friedel, H. O. Funsten, J. Goldstein, J. C. Green, A. Guthrie, M. G. Henderson, R. B. Horne, M. K. Hudson, J.-M. Jahn, V. K. Jordanova, S. G. Kanekal, B. W. Klatt, B. A. Larsen, X. Li, E. A. MacDonald, I. R. Mann, J. Niehof, T. P. OBrien, T. G. Onsager, D. Salvaggio, R. M. Skoug, S. S. Smith, L. L. Suther, M. F. Thomsen, and R. M. Thorne (2013), Science goals and overview of the energetic particle, composition, and thermal plasma (ECT) suite on NASAs Radiation Belt Storm Probes (RBSP) mission, *Space Sci. Rev.*, doi:10.1007/s11214-013-0007-5.

Su, Z., F. Xiao, H. Zheng, and S. Wang (2010), STEERB: A three-dimensional code for storm-time evolution of electron radiation belt, *J. Geophys. Res.*, *115*, A09,208, doi:10.1029/2009JA015210.

Su, Z., F. Xiao, H. Zheng, and S. Wang (2011a), CRRES observation and STEERB simulation of the 9 October 1990 electron radiation belt dropout event, *Geophys. Res.*

Lett., *38*, L06,106, doi:10.1029/2011GL046873.

Su, Z., F. Xiao, H. Zheng, and S. Wang (2011b), Radiation belt electron dynamics driven by adiabatic transport, radial diffusion, and wave-particle interactions, *J. Geophys. Res.*, *116*, A04,205, doi:10.1029/2010JA016228.

Su, Z., F. Xiao, H. Zheng, Z. He, H. Zhu, M. Zhang, C. Shen, Y. Wang, S. Wang, C. A. Kletzing, W. S. Kurth, G. B. Hospodarsky, H. E. Spence, G. D. Reeves, H. O. Funsten, J. B. Blake, and D. N. Baker (2014a), Nonstorm time dynamics of electron radiation belts observed by the Van Allen Probes, *Geophys. Res. Lett.*, *41*, 229–235, doi:10.1002/2013GL058912.

Su, Z., H. Zhu, F. Xiao, H. Zheng, Y. Wang, Q.-G. Zong, Z. He, C. Shen, M. Zhang, S. Wang, et al. (2014b), Quantifying the relative contributions of substorm injections and chorus waves to the rapid outward extension of electron radiation belt, *J. Geophys. Res. Space Physics*, *119*(12), 10,023–10,040, doi:10.1002/2014JA020709.

Su, Z., H. Zhu, F. Xiao, H. Zheng, Y. Wang, Z. He, C. Shen, C. Shen, C. B. Wang, R. Liu, M. Zhang, S. Wang, C. A. Kletzing, W. S. Kurth, G. B. Hospodarsky, H. E. Spence, G. D. Reeves, H. O. Funsten, J. B. Blake, D. N. Baker, and J. R. Wygant (2014c), Intense duskside lower band chorus waves observed by Van Allen Probes: Generation and potential acceleration effect on radiation belt electrons, *J. Geophys. Res.*, *119*(6), 4266–4273, doi:10.1002/2014JA019919.

Su, Z., H. Zhu, F. Xiao, H. Zheng, Y. Wang, C. Shen, M. Zhang, S. Wang, C. Kletzing, W. Kurth, et al. (2015), Disappearance of plasmaspheric hiss following interplanetary shock, *Geophys. Res. Lett.*, *42*(9), 3129–3140, doi:10.1002/2015GL063906.

Su, Z., Z. L. Gao, H. Zhu, W. Li, H. Zheng, Y. Wang, S. Wang, H. E. Spence, G. D. Reeves, D. N. Baker, J. B. Blake, H. O. Funsten, and J. R. Wygant (2016), Nonstorm time dropout of radiation belt electron fluxes on 24 September 2013, *J. Geophys. Res.*, *121*, 6400–6416, doi:10.1002/2016JA022546.

Subbotin, D., Y. Shprits, and B. Ni (2010), Three-dimensional VERB radiation belt simulations including mixed diffusion, *J. Geophys. Res.*, *115*, A03,205, doi: 10.1029/2009JA015070.

Summers, D., R. M. Thorne, and F. Xiao (1998), Relativistic theory of wave-particle resonant diffusion with application to electron acceleration in the magnetosphere, *J. Geophys. Res.*, *103*, 20,487, doi:10.1029/98JA01740.

Summers, D., C. Ma, N. P. Meredith, R. B. Horne, R. M. Thorne, D. Heynderickx, and R. R. Anderson (2002), Model of the energization of outer-zone electrons by whistler-mode chorus during the October 9, 1990 geomagnetic storm, *Geophys. Res. Lett.*, *29*(24), 240,000–1, doi:10.1029/2002GL016039.

Summers, D., B. Ni, and N. P. Meredith (2007), Timescales for radiation belt electron acceleration and loss due to resonant wave-particle interactions: 1. Theory, *J. Geophys. Res.*, *112*, A04,206, doi:10.1029/2006JA011801.

Summers, D., B. Ni, N. P. Meredith, R. B. Horne, R. M. Thorne, M. B. Moldwin, and R. R. Anderson (2008), Electron scattering by whistler-mode elf hiss in plasmaspheric plumes, *J. Geophys. Res.*, *113*, A04,219, doi:10.1029/2007JA012678.

Summers, D., Y. Omura, S. Nakamura, and C. A. Kletzing (2014), Fine structure of plasmaspheric hiss, *J. Geophys. Res.*, *119*(11), 9134–9149, doi:10.1002/2014JA020437.

Tao, X., Q. Lu, S. Wang, and L. Dai (2014), Effects of magnetic field configuration on the day-night asymmetry of chorus occurrence rate: A numerical study, *Geophys. Res. Lett.*, *41*, 6577–6582, doi:10.1002/2014GL061493.

Thorne, R. M. (2010), Radiation belt dynamics: The importance of wave-particle interactions, *Geophys. Res. Lett.*, *37*, L22,107, doi:10.1029/2010GL044990.

Thorne, R. M., E. J. Smith, R. K. Burton, and R. E. Holzer (1973), Plasmaspheric hiss, *J. Geophys. Res.*, *78*, 1581–1596, doi:10.1029/JA078i010p01581.

Thorne, R. M., S. R. Church, and D. J. Gorney (1979), On the origin of plasmaspheric hiss - The importance of wave propagation and the plasmapause, *J. Geophys. Res.*, *84*, 5241–5247, doi:10.1029/JA084iA09p05241.

Thorne, R. M., W. Li, B. Ni, Q. Ma, J. Bortnik, L. Chen, D. N. Baker, H. E. Spence, G. D. Reeves, M. G. Henderson, C. A. Kletzing, W. S. Kurth, G. B. Hospodarsky, J. B. Blake, J. F. Fennell, S. G. Claudepierre, and S. G. Kanekal (2013a), Rapid local acceleration of relativistic radiation-belt electrons by magnetospheric chorus, *Nature*, *504*, 411–414, doi:10.1038/nature12889.

Thorne, R. M., W. Li, B. Ni, Q. Ma, J. Bortnik, D. N. Baker, H. E. Spence, G. D. Reeves, M. G. Henderson, C. A. Kletzing, et al. (2013b), Evolution and slow decay of an unusual narrow ring of relativistic electrons near $L \sim 3.2$ following the september 2012 magnetic storm, *Geophys. Res. Lett.*, *40*, 3507C3511, doi:10.1002/grl.50627.

Tsurutani, B. T., and E. J. Smith (1974), Postmidnight chorus: a substorm phenomenon, *J. Geophys. Res.*, *79*, 118–127, doi:10.1029/JA079i001p00118.

Tsurutani, B. T., and E. J. Smith (1977), Two types of magnetospheric ELF chorus and their substorm dependences, *J. Geophys. Res.*, *82*, 5112–5128, doi: 10.1029/JA082i032p05112.

Tsurutani, B. T., O. P. Verkhoglyadova, G. S. Lakhina, and S. Yagitani (2009), Properties of dayside outer zone chorus during HILDCAA events: Loss of energetic electrons, *J. Geophys. Res.*, *114*, A03207, doi:10.1029/2008JA013353.

Tsurutani, B. T., B. J. Falkowski, J. S. Pickett, O. Santolik, and G. S. Lakhina (2014), Plasmaspheric hiss properties: observations from polar, *J. Geophys. Res.*, doi: 10.1002/2014JA020518.

Tsyganenko, N. A., and M. I. Sitnov (2005), Modeling the dynamics of the inner magnetosphere during strong geomagnetic storms, *J. Geophys. Res.*, *110*, A03,208, doi: 10.1029/2004JA010798.

Tu, W., G. S. Cunningham, Y. Chen, M. G. Henderson, E. Camporeale, and G. D. Reeves (2013), Modeling radiation belt electron dynamics during GEM challenge intervals with the DREAM3D diffusion model, *J. Geophys. Res.*, *118*, 6197–6211, doi: 10.1002/jgra.50560.

Varotsou, A., D. Boscher, S. Bourdarie, R. B. Horne, S. A. Glauert, and N. P. Meredith (2005), Simulation of the outer radiation belt electrons near geosynchronous orbit including both radial diffusion and resonant interaction with whistler-mode chorus waves, *Geophys. Res. Lett.*, *32*, L19,106, doi:10.1029/2005GL023282.

Varotsou, A., D. Boscher, S. Bourdarie, R. B. Horne, N. P. Meredith, S. A. Glauert, and R. H. Friedel (2008), Three-dimensional test simulations of the outer radiation belt electron dynamics including electron-chorus resonant interactions, *J. Geophys. Res.*, *113*, A12,212, doi:10.1029/2007JA012862.

Wygant, J., J. Bonnell, K. Goetz, R. Ergun, F. Mozer, S. Bale, M. Ludlam, P. Turin, P. Harvey, R. Hochmann, K. Harps, G. Dalton, J. McCauley, W. Rachelson, D. Gordon, B. Donakowski, C. Shultz, C. Smith, M. Diaz-Aguado, J. Fischer, S. Heavner, P. Berg, D. Malsapina, M. Bolton, M. Hudson, R. Strangeway, D. Baker, X. Li, J. Albert, J. Foster, C. Chaston, I. Mann, E. Donovan, C. Cully, C. Cattell, V. Krasnoselskikh, K. Kersten, A. Brenneman, and J. Tao (2013), The electric field and waves instruments on the radiation belt storm probes mission, *Space Sci. Rev.*, *179*(1-4), 183–220, doi:10.1007/s11214-013-0013-7.

Yang, C., Z. Su, F. Xiao, H. Zheng, Y. Wang, S. Wang, H. Spence, G. Reeves, D. Baker, J. Blake, and H. Funsten (2016), Rapid flattening of butterfly pitch angle distributions of radiation belt electrons by whistler-mode chorus, *Geophys. Res. Lett.*, *43*(16), 8339–8347, doi:10.1002/2016GL070194.

Zhou, C., W. Li, R. M. Thorne, J. Bortnik, Q. Ma, X. An, X.-j. Zhang, V. Angelopoulos, B. Ni, X. Gu, S. Fu, and Z. Zhao (2015), Excitation of dayside chorus waves due to magnetic field line compression in response to interplanetary shocks, *J. Geophys. Res.*, *120*, 8327–8338, doi:10.1002/2015JA021530.

Zhu, H., Z. Su, F. Xiao, H. Zheng, Y. Wang, C. Shen, T. Xian, S. Wang, C. Kletzing, W. Kurth, et al. (2015), Plasmatrough exohiss waves observed by Van Allen Probes: Evidence for leakage from plasmasphere and resonant scattering of radiation belt electrons, *Geophys. Res. Lett.*, *42*(4), 1012–1019, doi:10.1002/2014GL062964.

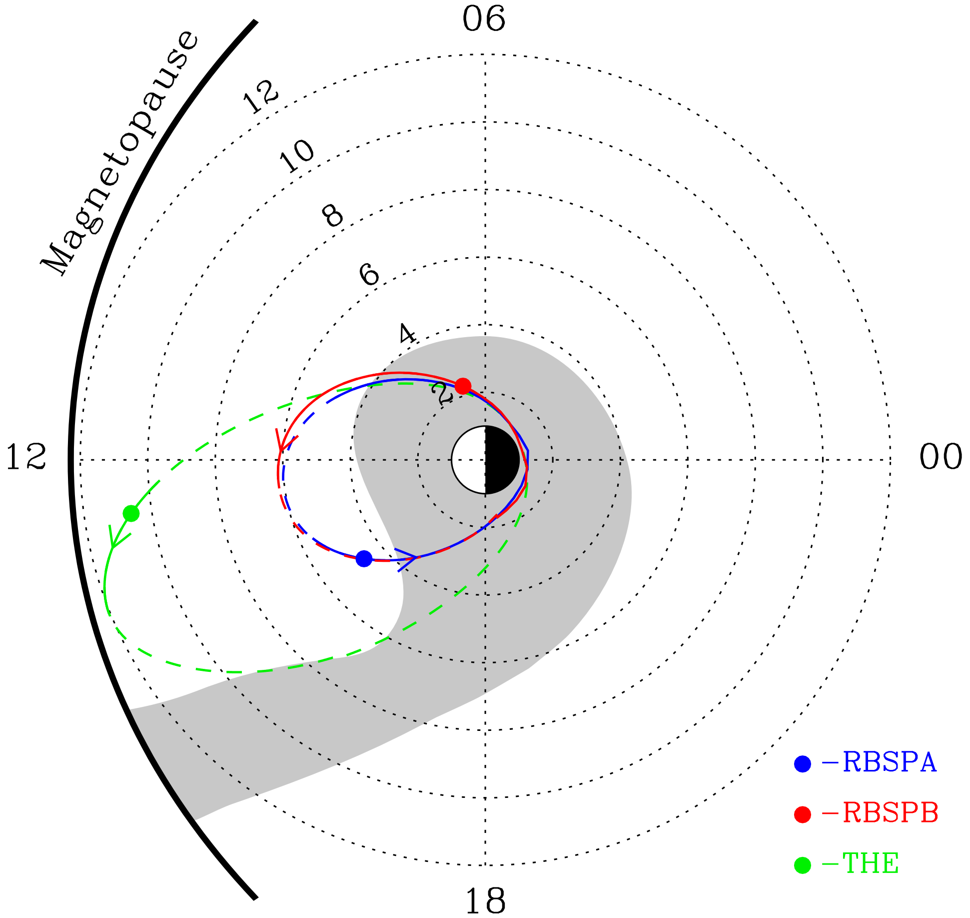

Figure 1. Orbits (dashed lines) of RBSP-A (blue), RBSP-B (red) and TH-E (green) satellites in the L–MLT plane on 12 February 2014. The solid lines correspond to the satellite trajectories in the time period from 03:00 UT to 08:00 UT. The solid dots, bold thick line, and gray shadow represent the locations of these satellites, the magnetopause and the plasmasphere around the pulse time, respectively.

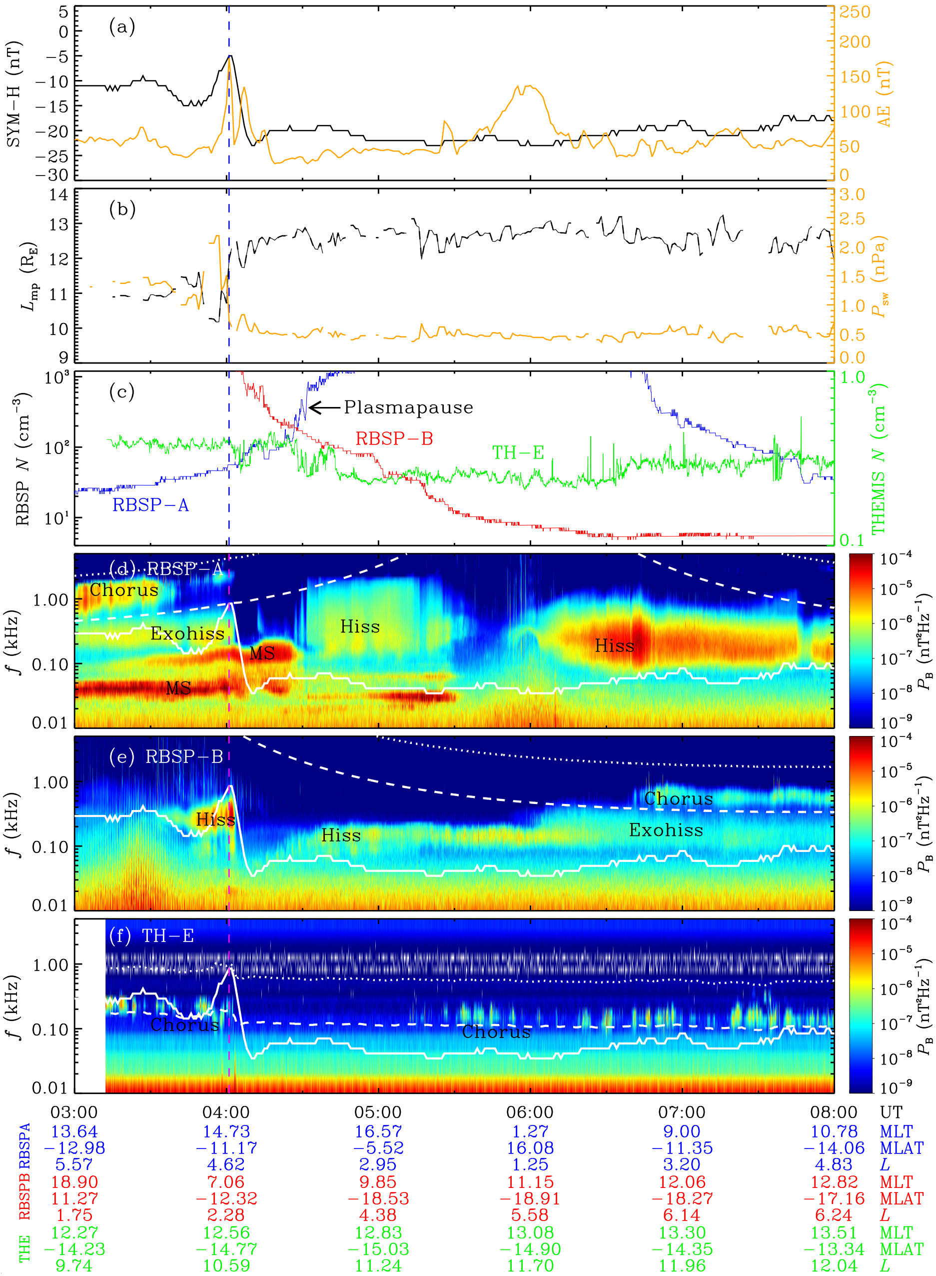

Figure 2. (a) Geomagnetic activity indices SYM-H and AE; (b) Location of subsolar magnetopause L_{mp} and solar wind dynamic pressure P_{sw}; (c) Cold electron densities N measured by RBSP-A, RBSP-B and TH-E satellites; (d-f) Magnetic field power spectral intensities P_B observed by RBSP-A, RBSP-B and TH-E satellites. In Figures 2d-f, the solid white lines represent the SYM-H indices. In Figures 2d-e, the dashed and dotted lines represent $0.1 f_{ce\_eq}$ and $0.5 f_{ce\_eq}$, where f_{ce_eq} is calculated as $f_{ce\_eq} = f_{ce} B_{Me}/B_{Mo}$ with the local electron gyrofrequency f_{ce} and the ratio B_{Me}/B_{Mo} between equatorial and local magnetic field strengthes in the TS04 model

[*Tsyganenko and Sitnov*, 2005]. In Figure 2f, the dashed and dotted lines represent $0.1 f_{ce}$ and $0.5 f_{ce}$. The vertical dashed line marks the arrival time of the solar wind negative pressure pulse.

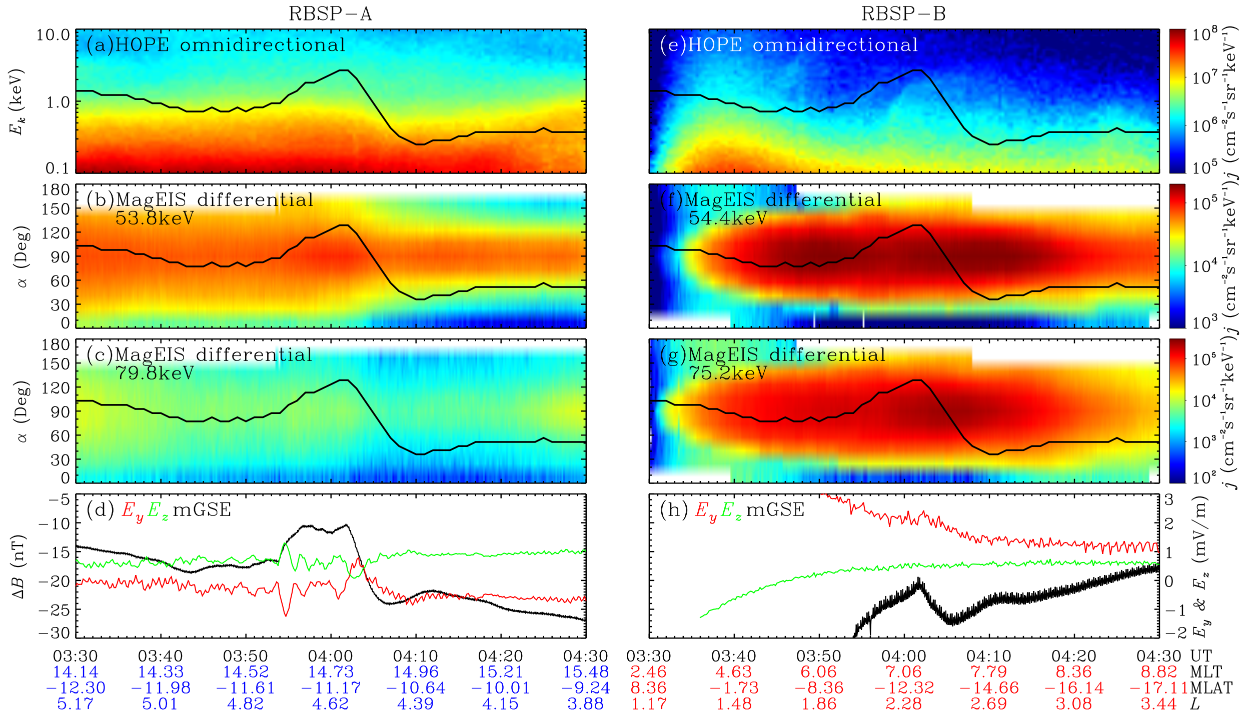

Figure 3. (a-c, e-g) Color-coded electron omnidirectional/differential fluxes j, (d, h) magnetic field variation ΔB (difference between the measured field and the International Geomagnetic Reference Field) and (d, h) electromagnetic field components E_y and E_z (in the the modified geocentric solar ecliptic coordinate system [*Wygant et al.*, 2013]) for twin RBSP satellites around the pulse time. In Figures 3a-c and 3e-g, the black lines represent the SYM-H indices.

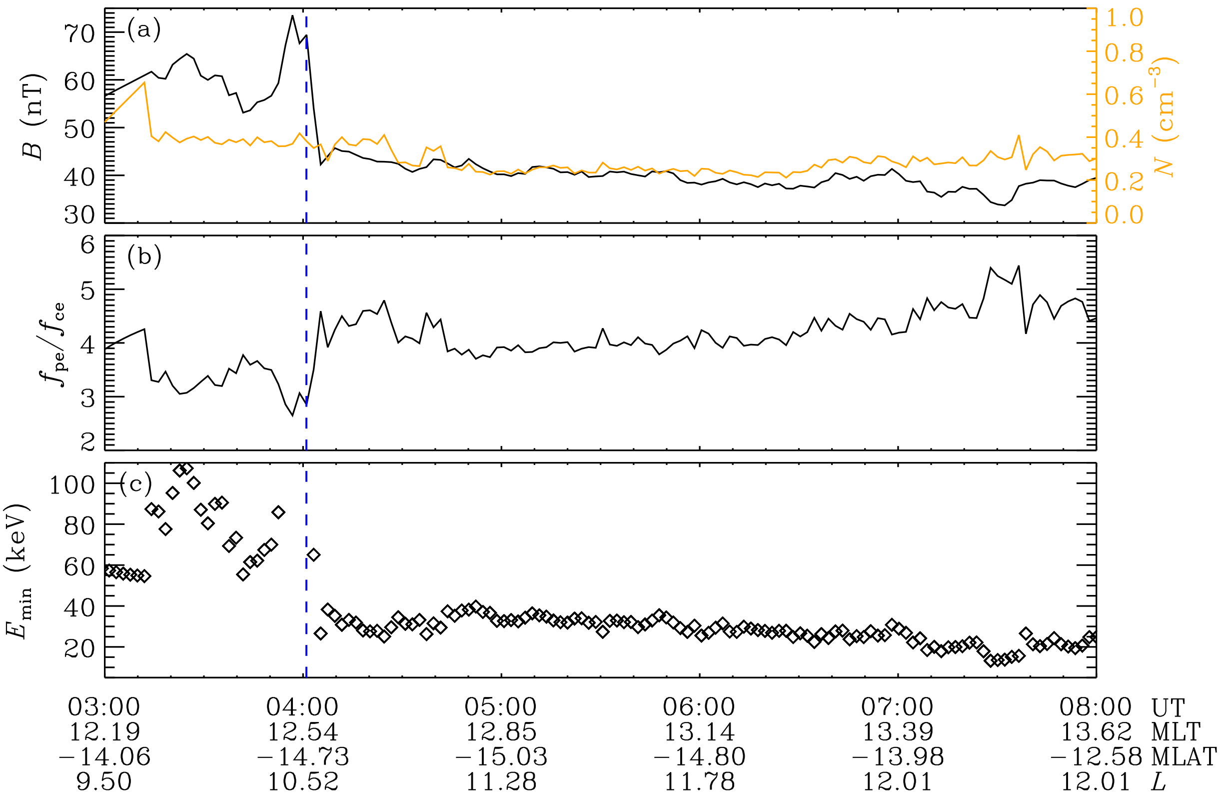

Figure 4. Temporal evolutions of (a) magnetic field strength B, (a) electron density N, (b) ratio between plasma frequency and electron gyrofrequency f_{pe}/f_{ce} and (c) minimum resonant energy E_{min} of chorus waves at the central frequency 0.25 kHz for TH-E satellite. The vertical dashed line represents the arrival time of the solar wind negative pressure pulse.

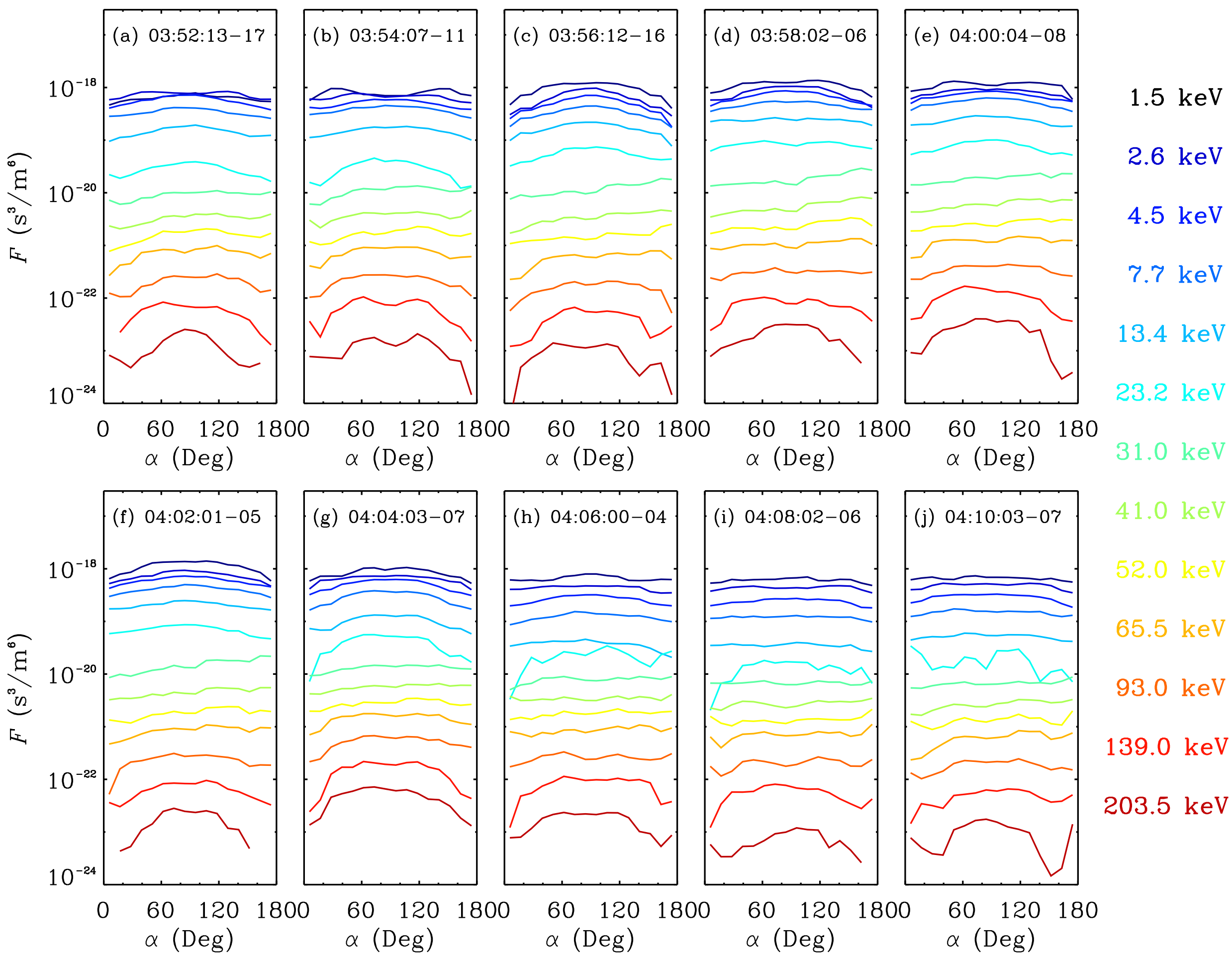

Figure 5. Temporal evolution of electron phase space densities for TH-E satellite during the time period from 03:52 UT to 04:10 UT.

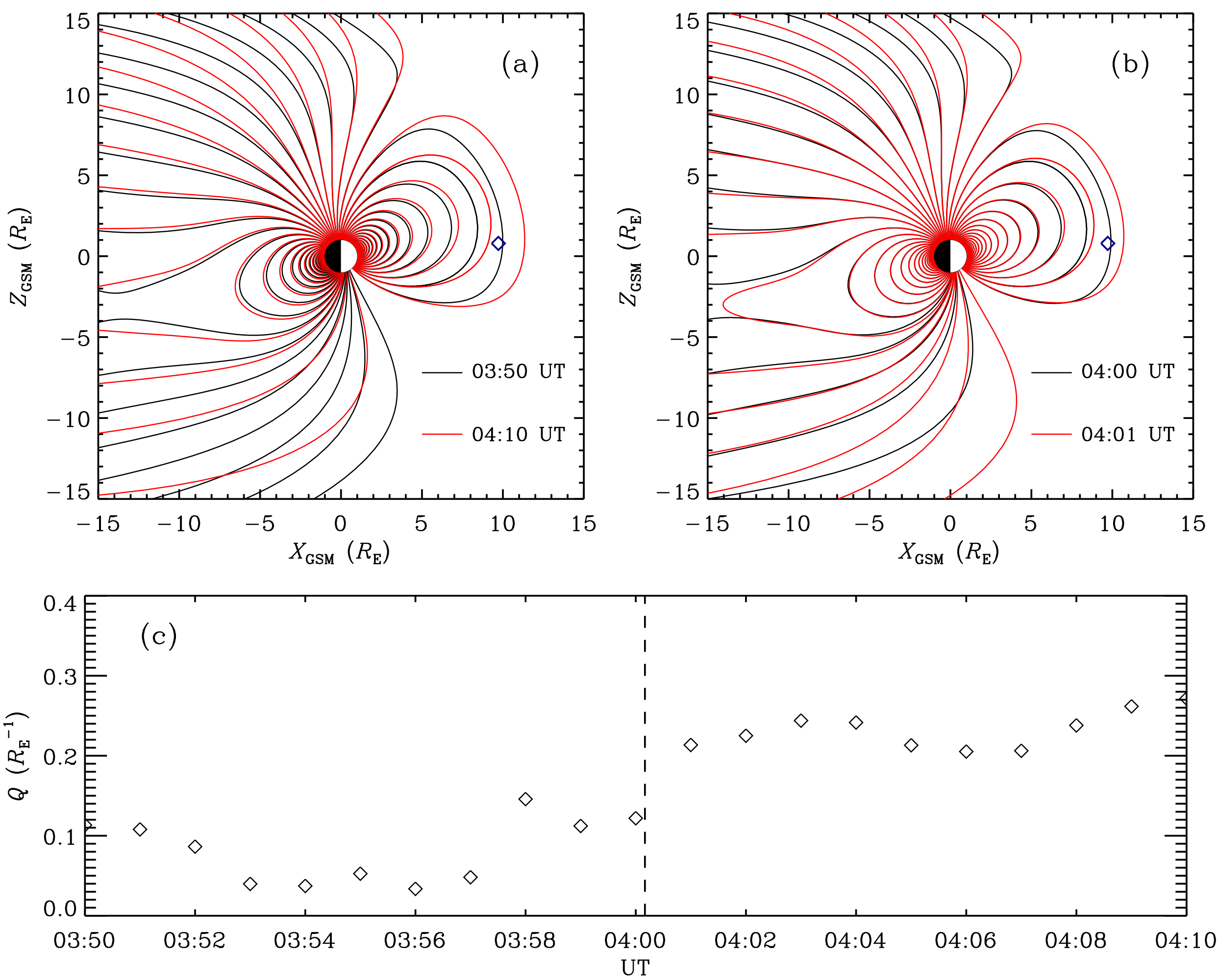

Figure 6. Comparisons of geomagnetic field configurations in the X–Z plane of the geocentric solar magnetospheric coordinate system on 20-min (a) and 1-min (b) timescales, with the diamond symbols denoting the TH-E satellite locations; (c) Temporal evolution of magnetic field line curvature Q for TH-E satellite, with the dashed line marking the arrival time of the solar wind negative pressure pulse.